



EVALUATION OF THE RADON RISK LEVEL FROM SOIL IN JIGAWA STATE, NIGERIA, USING A 10-POINT EVALUATION SYSTEM

Mansur, Z.,¹ Idris, A.,¹ Murtala, U.M.² and Mohammed, A.²

¹Department of Physics, Bayero University, Kano, Nigeria.

²Department of Geography, Bayero University, Kano, Nigeria

Email: manzangina1@gmail.com Phone No: +2347025433802,

ABSTRACT

In this research, a ten-point radon potential system was used in assessing and mapping the radon-prone area of Jigawa State, Nigeria. Radon is the second-highest cause of lung cancer mortality in the world. The increased lung cancer among non-smokers in Nigeria required a critical investigation of the cause. One way of achieving this is by identifying areas of high radon potential. The ten-point evaluation system uses a graded approach to assess radon areas as low, medium, or high potential zones. This system is applied to Jigawa state. It shows that 72.76% of Jigawa state has low radon potential, 27.24% has medium radon potential, and no area of Jigawa state has high radon potential. The total annual effective dose for low, medium, and high radon potential areas was calculated in the range of 0.276 mSvy⁻¹ to 2.758 mSvy⁻¹, 3.033 mSvy⁻¹ to 9.927 mSvy⁻¹, and 10.204 mSvy⁻¹ to 13.789 mSvy⁻¹, respectively. High radon potential levels indicate the upper bound of the maximum tolerable dose to individuals slated by the International Commission for Radiation Protection (ICRP). The findings of this study show that the people of Jigawa State are living at a safe level of radon exposure.

Key words; ArcGIS, annual effective dose, Radon Potential, Ten-point system

INTRODUCTION

Cancer is estimated to be an increasingly important cause of morbidity and mortality across the globe. The international agency for research on cancer (IARC) estimates that by 2030, over 24 million people will be diagnosed with cancer and 13 million will die from it every year. Radiation exposure from the radionuclides in the uranium and thorium decay series, together with the non-series potassium-40 nuclide, may contribute to this effect. However, exposure to these radiation sources causes stochastic health effects or non-stochastic health effects (Claus, 2010). Stochastic effects are associated with long-term, low-level exposure to radiation such as cancer and mutation. The non-stochastic health effects are associated with short-term, high-level exposure such as burns, radiation sickness, and death (Claus 2010). Radon, which decays through alpha emission and can be produced from uranium and thorium bearing minerals, which are common in the upper layer of the Earth's crust, was discovered to be the second-highest cause of lung cancer mortality apart from cigarette smoking (Darby *et al.*, 2001; Zeeb and Shannoun, 2010). This threat posed to health by radon is generating growing attention by national and international

authorities aimed at assessing the exposure of people to this radioactive gas and identifying those geographical areas where high radon potential is more likely to be found (Sarra *et al.*, 2016). Two approaches have been developed to minimize its effect and delineate the radon-prone areas. Some adopted an experimental design in which radon concentration in soil gas, underground drinking water, and indoor and outdoor air was used in the assessment and delineation of radon-prone areas. For instance, radon potential has been assessed and mapped into low, medium, and high potential in southwest England, Switzerland, Korea, northwest Spain, the southwestern part of Nigeria, and so on, using this approach (Varley and Flowers, 1998; Raybach *et al.*, 2002; Je *et al.*, 2007; Quindós *et al.*, 2008; Ajayi and Olubi, 2016; Ajiboye *et al.*, 2018). While others adopted a theoretical approach, investigation shows that there is strong statistical evidence that areal variation of radon levels depends on geological and other site-related parameters (Sarra *et al.*, 2016; Kemski *et al.*, 1992; Kemski *et al.*, 1996; Al-Tamimi and Abumurad, 2001; Adepelumi *et al.*, 2005; Kemski *et al.*, 2009; Watson *et al.*, 2017).

Special Conference Edition, April, 2022

Hence, many scientists consider these parameters and have developed many models or systems that can be used to assess and map radon-prone areas. For instance, radon potential has been assessed and mapped into low, medium, and high potentials using a ten-point evaluation system in Germany and Hong Kong, China (Bleile and Wiegand, 2005; Tung *et al.*, 2013) and using geostatistical simulations with a nested model in Italy (Cafaro *et al.*, 2016). Recent research has shown a sharp increase in reported cases of lung cancer among non-smokers, which may be traceable to the ingestion and inhalation of ^{222}Rn in underground drinking water and indoor and outdoor air (Ezemba *et al.*, 2012; Ajiboye *et al.*, 2018). However, due to the inadequate data for radon potential zones in Nigeria that can resolve the spatial distribution of radon-prone areas and difficulties arising due to the lack of accessibility of radon detectors, a new method of producing radon potential maps is, however, pertinent to be explored. In this research, therefore, a ten-point radon potential system was used in assessing and mapping the radon-prone areas of Jigawa State, Nigeria. The system was proposed by Wiegand (2001), while the validation of the system was done by Bleile and Wiegand (2005), who presented figures of soil radon potential and concentration mainly from Quaternary to Cretaceous materials in Germany, which showed strong correlations between experiment and the 10-point radon potential system. Similarly, a correlation was also found between the 10-point radon potential and the soil radon concentration in Hong Kong, China, particularly in the places of relatively homogenous geology with the medium value of radon potential in their effort to revalidate the system (Tung *et al.*, 2013).

MATERIALS AND METHODS

Sampling Area

The study area lies between Latitudes 11.000°N to 13.000°N and Longitudes 8.000°E to 10.150°E in the North-West geopolitical zone of Nigeria, with an area of approximately 23154Km^2 and about 3.6 million inhabitants. It shares a border to the south and east with Bauchi State to the east and north with Yobe State; and to the west with Kano and the Katsina States. It also shares an international boundary to the north with the Niger Republic and characterized by undulating land with several Dunes of various sizes spanning several kilometers. While the southern part comprises mainly the basement complex, also to the northeast is made up of sedimentary rocks of

the Chad formation and characterized by semi-arid climate with long dry season and a short wet season and indicating a variables climate with erratic and vary considerably over the course of the year. Most of the area lies within the Sudan Savannah, with an element of the Guinea Savannah in the south (Abdullahi *et al.*, 2016).

A List of Materials

1. Geological map of the study areas
2. Shuttle radar topographic mission data
3. Land use data
4. State boundary map of Nigeria
5. ArcGIS Software
6. Laptop computer

A 10-Point Radon Potential System

The system involves the inspection of in situ geogenic and anthropogenic factors such as geology, relief, vegetation cover, tectonics, soil sealing, and traffic vibrations (Table 1) and assessing each of the sampling sites or geological units with points of the five controlling parameters and summing up all the points in each sample site. The resulting score ranges from 0 to 10 points, whereby 0 represents low radon potential, 3 represents medium radon potential, and 4 represents high radon potential, respectively.

As long as only the soil radon in rural and natural areas is concerned, the effects of traffic vibration and soil sealing are not considered in this study. This is because the study area was characterized as a rural area and the impact of vibrations on soil gas radon concentration was studied by Schmid and Wiegand (1998) and found that the strongest vibrations and the most striking impact on the ^{222}Rn concentrations in soil gas were observed in the vicinity of construction sites. In particular, when metal panels were rammed into the ground, a doubling of ^{222}Rn concentrations close to the vibration source was measured. Even at a distance, the concentrations were increased by about 30%. Much weaker vibrations were generated by road traffic, which resulted in a smaller effect on soil ^{222}Rn potential. Hence, it should be neglected.

Similarly, sealing of soils results in a reduction of exhalation but an increase in ^{222}Rn concentrations beneath the sealing. It is well known that natural soil sealing by frost and snow cover has no effect in the study areas, and an investigation conducted by Wiegand and Schott (1999) and Wiegand (2001) shows that the effect of artificial sealing (e.g., roads, squares, and buildings) is very high in urban areas and very low in rural areas. Hence, it can also be neglected.

Origin of Soil Data analysis

The study area was characterized as rural, land used data of Nigeria and the clip layer of the study area was inputted into ArcMap software, and the data were thoroughly investigated, but no backfill was discovered in the study area. Hence, it was considered undisturbed.

Geology Data Analysis

The state boundary map of Nigeria and the geological map of the study area were inputted and the geological map was georeferenced to match its exact geographic location. Two parameters were assessed using this georeferenced geological map; fault and variety of rocks.

Variety of Rocks

The variety of rocks was assessed based on the dominant category of rocks in each geological unit and where there are two varieties of rocks

belonging to two different categories, the geological unit was assessed with the point of a variety of rocks having high points. The point of undisturbed was added to the assessed field of the variety of rocks on the geological map. The vector map was converted into a raster with the assessed field. This implies that the raster map obtained contains the point of undisturbed and the points of the variety of rocks cumulatively. Then, the raster map and polygon shapefile were unchecked leaving the georeferenced geological map.

Local Parameter (Fault)

A new shapefile for digitization was created and then the fault lines in the geological map were digitized into a polyline and then a new field was added in the attribute table of the shapefile and the point of fault was assigned in the field. Then, the shapefile was converted into a density map.

Table 1: Ten Point Radon Potential System (Tung *et al.*,2013)

SN	Parameters	Rating Points	
1	Origin of soil	(1) undisturbed soil or backfill<2 m (go to 2.1)	2
		(2) backfill>2 (go to 2.2)	0
2	Geology	2.1 Variety of rocks	
		Sediment: black shale, phosphorite, bauxite	3
		Magmatic rock: (a) silicic rocks (e.g. granite, granodiorite, syenite, monzonite, Rhyolite, rhyolite lava, dacite, pumice, pegmatite), (b) Alkaline rocks (e.g. phonolite, nephelinite)	
		Volcanic rock: crystal tuff	
		Metamorphic rock: orthogneiss, greisen	1
		Sediment: gravel, clay, pelite, carbonate rock, loess, mudstone, Metasiltsone, metaconglomerate, metasandstone, eutaxite	
		Magmatic rock: intermediate rocks (e.g. diorite, andesite)	
		Volcanic rock: trachyte, tuff, tuffite	
		Metamorphic rock: clay schist, mica schist, paragneiss, granulite, marble	0
		Sediment: sand, sandstone, conglomerate, evaporite, silstone, silicified sandstone	
		Magmatic rock: (a) mafic rocks (e.g. gabbro, basalt, diabase) (b) ultramafic rocks (e.g. peridotite)	
		Metamorphic rock: quartzite, amphibolite, eclogite, serpentinite, metasediments	
	2.2 Type of back fill		
	High226 Ra conc.: slags, ashes, sewage sludge, tailings (ore mining)	3	
	Low226 Ra conc.: sand, gravel, soil aggradation, rubble, tailings(coal mining)	0	
3	Relief	Upper part of hill	1
		Lower part of hill	0
		Plain	0
4	Vegetation	Grass, field, meadow or no vegetation	1
		Forest, bush, scrub, mixed plantation	0
5	Local Parameters	Tectonic elements: fault, mining subsidence	1
		Soil sealing>50 % e.g. urban area	1
		Strong traffic vibration (trains or trucks)<10 m distance	1
		Maximum points	10

Special Conference Edition, April, 2022
Shuttle Radar Topographic Mission (SRTM)
Data Analysis

The SRTM of Nigeria was imported then the relief map of the study area was extracted. The extracted relief map was reclassified into three (3) using Reclassify and then a new field was added to the attribute table of reclassified relief map. The smallest range class was assigned the point of plain land, the medium-range class was assigned the point of a lower part of the hill and the highest range class was assigned the point of the upper part of the hill.

Land Use Data Analysis

The clipped land used data of the study area was displayed and then, a new field was added in the attribute table where the vegetation was assessed based on the dominant variety of

vegetation in each geological unit. Finally, the vector map of the study area was converted into a raster map.

Weighted Sum

The weighted sum was used in summing the four assessed raster maps with their assessed field into a single map that contains all the information from other maps. This single map was reclassified into low, medium, and high radon potential using reclassify. The final map obtained is the radon potential map.

RESULT AND DISCUSSION

After assessing the variety of rocks together with origin of soil, fault, relief and vegetation cover, the following results were obtained and shown in figure 1-4.

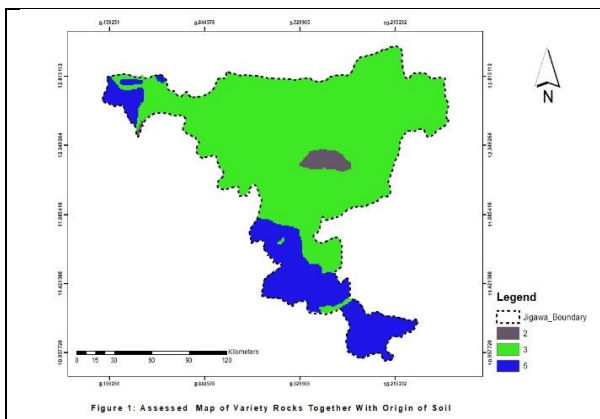


Figure 1: Assessed Map of Variety of Rocks Together with Origin of Soil

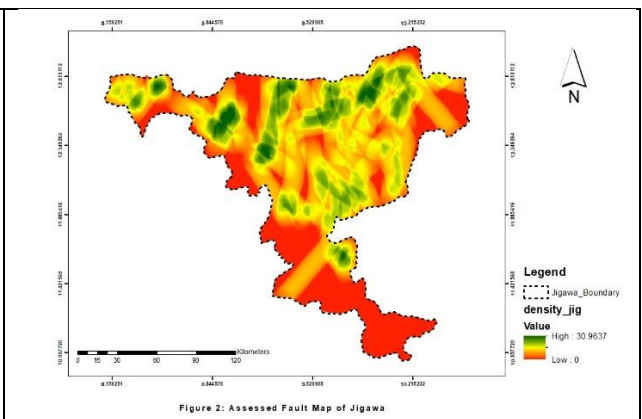


Figure 2: Assessed Fault Map of Jigawa

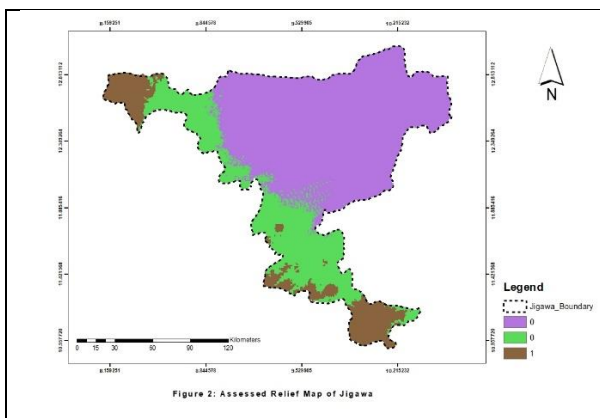


Figure 3: Assessed Relief Map of Jigawa

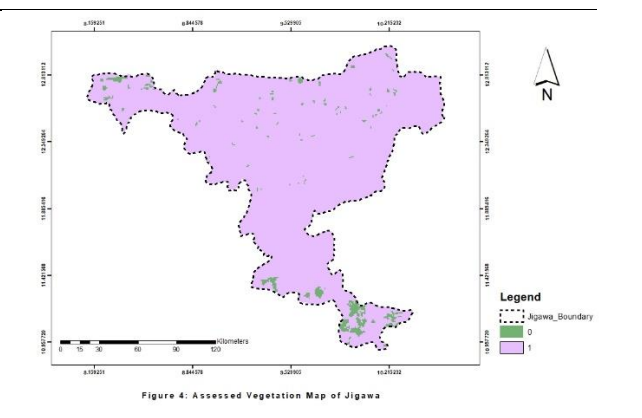


Figure 4: Assessed Vegetation Map of Jigawa

After summing the above raster data and classify the results into low, medium and high. The following final radon potential map was obtained

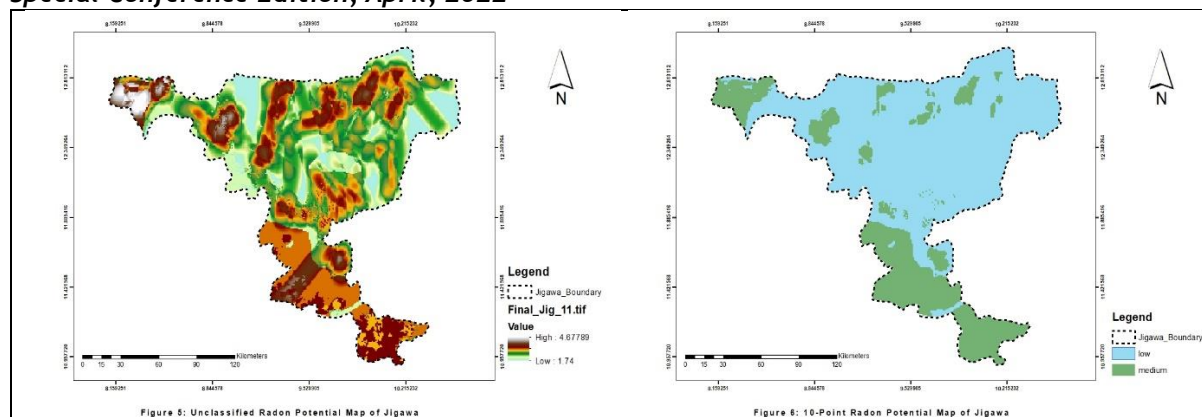


Figure 5: Unclassified Radon Potential Map of Jigawa

Figure 6: 10-Point Radon Potential Map of Jigawa

Table 2: 10-Point Radon Potential Areas

Radon Potential	Low (Km ²)	%	Medium (Km ²)	%
Land Mass	16848	72.76	6306	27.24

Table: 2 shows land mass occupied by low and medium radon potential with their percentage in a ten-point radon potential analysis, while Fig: 6, the radon potential map, points to areas, where, in unfavorable cases, high radon potential is likely to occur, and on the other hand, helps to identify

regions of exclusion. It was found that 72.76% of Jigawa state was occupied by low radon potential and 27.24% was occupied by medium radon potential, while no area of Jigawa state was occupied by high radon potential.

Indoor Radon Concentration Level Prediction Corresponds to 10-Point System Classification

Although the risk to tissues posed by radon can occur through ingestion of water with a high radon concentration, it's much smaller than that associated with inhalation exposure to radon. The International Commission of Radiological Protection (ICRP) considered that simple counter measures would be virtually certain to be justified to avert an effective dose of 10mSv in a year (i.e. the upper bound of the maximum tolerable dose to individuals) and a yearly average radon concentration of 200Bqm⁻³ —600Bqm⁻³. Similarly, ICRP recommended a radon concentration of 600Bqm⁻³ as that at which action is almost certain to be justified and it expected optimization to suggest an action level not lower than 200Bqm⁻³. While the World Health Organization (WHO), established a national annual average concentration reference level of 100Bqm⁻³ but said that "if this level cannot be reached under the prevailing country specific conditions, the level should not exceed 300Bqm⁻³". Bearing this in mind, radon content in soil gave more accurate indoor radon predictions than external gamma radiation or ²²⁶Ra concentration in soil, and the level of indoor radon concentration was far greater than outdoor

radon concentration (Wiegand, 2001;Quindós *et al.*, 2008;Tung *et al.*, 2013;Watson *et al.*, 2017). From the above statements made by ICRP and WHO, the indoor radon concentration classification that corresponds to the 10-point radon potential classification and soil gas radon concentration classification can be predicted as [Rn] < 100Bqm⁻³ for low, 100Bqm⁻³ < [Rn] < 360Bqm⁻³ for medium and [Rn] > 360Bqm⁻³ for high indoor radon potential. This predicted indoor radon level can be validated by using the total annual effective dose and considering the ratio of indoor to outdoor radon concentration used in (UNSCEAR, 2000).

To calculate the total annual effective dose for low, medium, and high radon potential areas with an indoor/outdoor radon concentration ratio of 4:1, the dose conversion coefficient 9nSv (Bq h m⁻³)⁻¹, indoor and outdoor equilibrium factors of 0.4 and 0.6, and indoor and outdoor occupancy factors of 7000hy⁻¹ and 1760hy⁻¹, proposed by (UNSCEAR, 2000), must be used. Therefore, the annual effective dose is determined as follows:

$$Indoor(mSvy^{-1}) = C_{Rn}(Bqm^{-3}) \times 0.4 \times 7000hy^{-1} \times 9nSv (Bq h m^{-3})^{-1} \times 10^{-6} \quad (1)$$

$$Outdoor(mSvy^{-1}) = C_{Rn}(Bqm^{-3}) \times 0.6 \times 1760hy^{-1} \times 9nSv (Bq h m^{-3})^{-1} \times 10^{-6} \quad (2)$$

Table 4: The calculated indoor, outdoor and total annual effective dose for low, medium and high radon potential areas

Radon Level	Radon (Bqm ⁻³)	concentration		Annual Effective Dose (mSvy ⁻¹)		Total (mSvy ⁻¹)	AED
	Indoor	Outdoor	Indoor	Outdoor			
Low	10	2.5	0.252	0.024	0.276		
	50	12.5	1.26	0.119	1.379		
	100	25	2.52	0.238	2.758		
Average	53.3	13.3	1.343	0.126	1.469		
Medium	110	27.5	2.772	0.261	3.033		
	200	50	5.04	0.475	5.515		
	360	90	9.072	0.855	9.927		
Average	223.3	55.8	5.627	0.53	6.157		
High	370	92.5	9.324	0.879	10.204		
	400	100	10.08	0.95	11.03		
	500	125	12.6	1.188	13.789		
Average	423.3	105.8	10.667	1.006	11.673		

This implies that the people living in low radon potential areas received total annual effective dose in the range of 0.276 mSvy⁻¹ to 2.758 mSvy⁻¹ with an average of 1.469 mSvy⁻¹ which is far more below the upper bound of the maximum tolerable dose to individuals. The people living in medium radon potential areas received total annual effective dose in the range of 3.033 mSvy⁻¹ to 9.927 mSvy⁻¹ with an average of 6.157mSvy⁻¹ which is also below the upper bound of the

maximum tolerable dose to individuals. Whereas the people living in high radon potential areas received total annual effective dose in the range of 10.204 mSvy⁻¹ to 13.789mSvy⁻¹ with an average of 11.673 mSvy⁻¹ which is above the upper bound of the maximum tolerable dose to individuals slated by ICRP, hence this total annual effective assessment validate the indoor radon concentration classification prediction.

CONCLUSION

Investigation of the radon potential zone is necessary to assure safety against the harmful effects of ionization radiation in a specific environment. The ten-point radon potential system was used in assessing the radon-prone areas of Jigawa State, Nigeria. It was found that 72.76% of Jigawa state was occupied by low radon potential, 27.24% was occupied by medium radon potential, and no area of the state was occupied by high radon potential. the people living in low radon potential areas received an average annual effective dose of 1.469 mSvy⁻¹ which is far below the upper bound of the maximum tolerable dose to individuals. The

people living in medium radon potential areas received an average annual effective dose of 6.157mSvy⁻¹ which is also below the upper bound of the maximum tolerable dose to individuals as slated by ICRP.

The results of this research show that the people of Jigawa State are living under the safety level of radon exposure. This research will serve as the foundation for providing the most recent levels of radiation data of various locations in Jigawa state, which can be attributed to the fact that the majority of the state's land mass was occupied by sedimentary rocks with a basement complex element.

REFERENCES

- Abdullahi, S., Ndikilar, C. E., Suleiman, A. B., and Y.Hafeez, H. (2016). Assessment of Heavy Metals and Radioactivity Concentration in Drinking Water Collected From Local Wells and Boreholes of Dutse Town, North West, Nigeria. *Journal of Environment Pollution and Human Health*, 4(1): 1–8. <https://doi.org/10.12691/jephh-4-1-1>
- Adepelumi, A. A., Ajayi, T. R., Ako, B. D., and Ojo, A. O. (2005). Radon soil–gas as a geological mapping tool: case study from basement complex of Nigeria. *Environmental Geology*, 48(6): 762–770. <https://doi.org/10.1007/s00254-005-0016-0>
- Ajayi, O. S., and Olubi, O. E. (2016). Investigation of indoor radon levels in some dwellings of southwestern Nigeria. *Environmental Forensics*, 17(4): 275–281.

Special Conference Edition, April, 2022

- <https://doi.org/10.1080/15275922.2016.1230909>
- Ajiboye, Y., Isinkaye, M. O., and Khanderkar, M. U. (2018). Spatial distribution mapping and radiological hazard assessment of groundwater and soil gas radon in Ekiti State, Southwest Nigeria. *Environmental Earth Sciences*, 77(14): 1–15. <https://doi.org/10.1007/s12665-018-7727-5>
- Al-Tamimi, M. H., and Abumurad, K. M. (2001). Radon anomalies along faults in North of Jordan. *Radiation Measurements*, 34(1–6): 397–400. [https://doi.org/10.1016/S1350-4487\(01\)00193-7](https://doi.org/10.1016/S1350-4487(01)00193-7)
- Bleile, D., and Wiegand, J. (2005). Checking the “10 point system” for an evaluation of the soil radon potential. *Radioactivity in the Environment*, 7(C): 833–841. [https://doi.org/10.1016/S1569-4860\(04\)07104-9](https://doi.org/10.1016/S1569-4860(04)07104-9)
- Cafaro, C., Giovani, C., and Garavaglia, M. (2016). Geostatistical simulations for radon indoor with a nested model including the housing factor. *Journal of Environmental Radioactivity*, 151, 264–274. <https://doi.org/10.1016/j.jenvrad.2015.10.002>
- Claus, G. (2010). *Introduction to Radiation Protection* (H. Eugene Stanley, Ed.). <https://doi.org/10.1007/978-3-642-02586-0>
- Darby, S., Hill, D., and Doll, R. (2001). Radon: A likely carcinogen at all exposures. *Annals of Oncology*, 12: 1341–1351.
- Ezema, N., Ekpe, E. E., and Eze, J. C. (2012). Challenges of lung cancer management in a developing country. *Nigerian Journal of Medicine: Journal of the National Association of Resident Doctors of Nigeria*, 21(2): 214–217. Retrieved from www.researchgate.net/publication/234120380_Challenges
- Je, H. K., Kang, C. G., Choi, J. Y., Lee, J. S., and Chon, H. T. (2007). Assessment of soil and soil-gas radon activity using active and passive detecting methods in Korea. *Environmental Geochemistry and Health*, 29(4): 295–301. <https://doi.org/10.1007/s10653-007-9098-9>
- Kemski, J., Klingel, R., Schneiders, H., Siehl, R., and Wiegand, J. (1992). Geological Structure and Geochemistry Controlling Radon in Soil Gas. *Radiation Protection Dosimetry*, 45(1/4): 235–239.
- Kemski, J., Klingel, R., and Siehl, A. (1996). Classification and mapping of radon-affected areas in Germany. *Environment International*, 22(SUPPL. 1): 4120(96)00185-7. [https://doi.org/10.1016/S0160-4120\(96\)00185-7](https://doi.org/10.1016/S0160-4120(96)00185-7)
- Kemski, J., Klingel, R., Siehl, A., and Valdivia-Manchego, M. (2009). From radon hazard to risk prediction-based on geological maps, soil gas and indoor measurements in Germany. *Environmental Geology*, 56(7): 1269–1279. <https://doi.org/10.1007/s00254-008-1226-z>
- Quindós, L. S., Fernández, P. L., Sainz, C., Fuente, I., Nicolás, J., Quindós, L., and Arteche, J. (2008). Indoor radon in a Spanish region with different gamma exposure levels. *Journal of Environmental Radioactivity*, 99(10): 1544–1547. <https://doi.org/10.1016/j.jenvrad.2007.12.011>
- Rybach, L., Bächler, D., Bucher, B., and Schwarz, G. (2002). Radiation doses of Swiss population from external sources. *Journal of Environmental Radioactivity*, 62(3): 277–286. [https://doi.org/10.1016/S0265-931X\(01\)00169-2](https://doi.org/10.1016/S0265-931X(01)00169-2)
- Sarra, A., Fontanella, L., Valentini, P., and Palermi, S. (2016). Quantile regression and Bayesian cluster detection to identify radon prone areas. *Journal of Environmental Radioactivity*, 164, 354–364. <https://doi.org/10.1016/j.jenvrad.2016.06.014>
- Schmid, S., and Wiegand, J. (1998). The influence of traffic vibrations on the radon potential. *Health Physics*, 74(2): 231–236. <https://doi.org/10.1097/00004032-199802000-00008>
- Tung, S., Leung, J. K. C., Jiao, J. J., Wiegand, J., and Wartenberg, W. (2013). Assessment of soil radon potential in Hong Kong, China, using a 10-point evaluation system. *Environmental Earth Sciences*, 68(3): 679–689. <https://doi.org/10.1007/s12665-012-1782-0>
- UNSCEAR. (2000). *2000-Sources and Effects of Ionizing Radiation: Volume I*. <https://doi.org/10.1097/00004032-199907000-00007>
- Varley, N. R., and Flowers, A. G. (1998). Indoor radon prediction from soil gas measurements. *Health Physics*, 74(6): 714–718.

Special Conference Edition, April, 2022

- <https://doi.org/10.1097/00004032-199806000-00009>
- Watson, R. J., Smethurst, M. A., Ganerød, G. V., Finne, I., and Rudjord, A. L. (2017). The use of mapped geology as a predictor of radon potential in Norway. *Journal of Environmental Radioactivity*, 166: 341–354.
<https://doi.org/10.1016/j.jenvrad.2016.05.031>
- Wiegand, J. (2001). A guideline for the evaluation of the soil radon potential based on geogenic and anthropogenic parameters. *Environmental Geology*, (40): 949–963.
<https://doi.org/DOI.10.1007/s002540100287>
- Wiegand, J., and Schott, B. (1999). The sealing of soils and its effect on soil-gas migration. *Nuovo Cimento Della Societa Italiana Di Fisica C*, 22(3–4): 449–455.
- Wikipedia, (1991). Geology and Geographic information of Jigawa State, Retrieved from http://en.m.wikipedia.org/wiki/Jigawa_State
- Zeeb, H., and Shannoun, F. (2010). Indoor Radon a Public Health Perspective. *International Journal of Environmental Studies*, 67(1): 108.
<https://doi.org/10.1080/00207230903556771>